Korean J. Chem. Eng., 32(9), 1902-1909 (2015)
DOI: 10.1007/s11814-014-0393-8

pISSN: 0256-1115
eISSN: 1975-7220

Fabrication of composite nanofiltration membranes with enhanced structural stability for concentrating oligomeric proanthocyanidins in ethanol aqueous solution

Yanyan Ma*,, Yanlei Su*,**,†, Yafei Li*,**, and Zhongyi Jiang*,****

*Key Laboratory for Green Technology of Ministry of Education, School of Chemical Engineering and Technology, Tianjin University, Tianjin 300072, China
**Collaborative Innovation Center of Chemical Science and Engineering (Tianjin), Tianjin 300072, China
(*Received 18 November 2014 • accepted 28 December 2014*)

Abstract−Composite nanofiltration (NF) membranes with enhanced structural stability were fabricated and used to concentrate oligomeric proanthocyanidins (OPC) in ethanol solution. The composite NF membranes were prepared by interfacial polymerization of piperazine (PIP) with trimesoyl chloride (TMC), upon the porous supports of polyethersulfone (PES) and polyvinyl formal (PVF) blend membranes. The active layers of composite NF membranes were covalently linked to porous supports owing to hydroxyl groups of PVF upon support surface, which could participate in the interfacial polymerization reaction. The pure water fluxes of the composite NF membranes reached 34.9 L/m^2h, while the rejections of Na_2SO_4 and orange GII were 92.7% and 98.4%, respectively. The enhanced structural stability of the composite NF membranes were confirmed by long-term immersion experiment in ethanol. NF concentration process was considered as a potential alternative to conventional evaporation concentration process for OPC concentration in ethanol solution.

Keywords: Polyvinyl Formal (PVF), Composite Nanofiltration Membrane, Structural Stability, Oligomeric Proanthocyanidins (OPC), Concentration

INTRODUCTION

Nanofiltration (NF), which exhibits separation characteristics in the intermediate range between reverse osmosis (RO) and ultrafiltration (UF), has gained worldwide interest because of advantages such as low energy consumption, low operating cost and exceptional separation performance. The NF process has been widely applied in sewage treatment, drinking water production, seawater desalination and industrial substances separation [1-4]. Most commercial NF membranes are thin film composite membranes fabricated by interfacial polymerization, comprising thin active layers that dominate membrane performance (permeability and selectivity) and porous support layers that provide the mechanical strength of the composite membranes. The active layers formed by interfacial polymerization are always physically adhered on the supports. Although the composite NF membranes have exhibited good long-term stability in aqueous feeds, the structural stability should be reconsidered to enhance when the composite NF membranes are applied into harsh conditions, such as feed solutions containing ethanol which are enable swelling of active layers and supports seriously. The different degree in swelling and the weak interactions between these two layers would cause the peeling of active layers from supports during long-time operation, seriously damaging separation performance of composite NF membranes [5]. Therefore, it is important to build a robust interface between active layers and supports of composite NF membranes.

Several studies have tried some strategies to enhance the interfacial adhesion of composite NF membranes [6-10]. Zhao et al. modified polyethersulfone (PES) supports with polydopamine "before" carrying out interfacial polymerization to prepare composite NF membranes. The interaction between the active layer and the support of the composite NF membrane was enhanced due to the bioadhesion of polydopamine [6]. Polyacrylonitrile (PAN) supports were hydrolyzed to create carboxyl groups on surfaces, which were then activated to enhance reactivity with amine groups, for preparing polyamide (PA) NF membranes with high separation performance [10]. As a big challenge to increase the structural stability of composite NF membranes, other facile methods deserve to be explored for fabricating structural stable composite NF membranes.

Surface segregation has evolved as a facile and effective approach to introduce hydrophilic groups onto UF membranes surface and improve their hydrophilicity [11-15]. The introduction of functional groups via surface segregation could react with active layers onto the supports, which may be a facile approach capable of enhancing the structural stability of composite NF membranes. In this study, polyethersulfone (PES) and polyvinyl formal (PVF) were blended to prepare porous supports. PA active layers were formed by interfacial polymerization of piperazine (PIP) with trimesoyl chloride (TMC). The hydroxyl groups of PVF were enriched on the surface of the supports via surface segregation, which would react with acid chloride groups of TMC molecules and form ester bonds during interfacial polymerization. A schematic illustration for the formation of covalent bond of the composite NF membranes is presented in Fig. 1. The structural stability of the composite NF membranes

†To whom correspondence should be addressed.
E-mail: suyanlei@tju.edu.cn

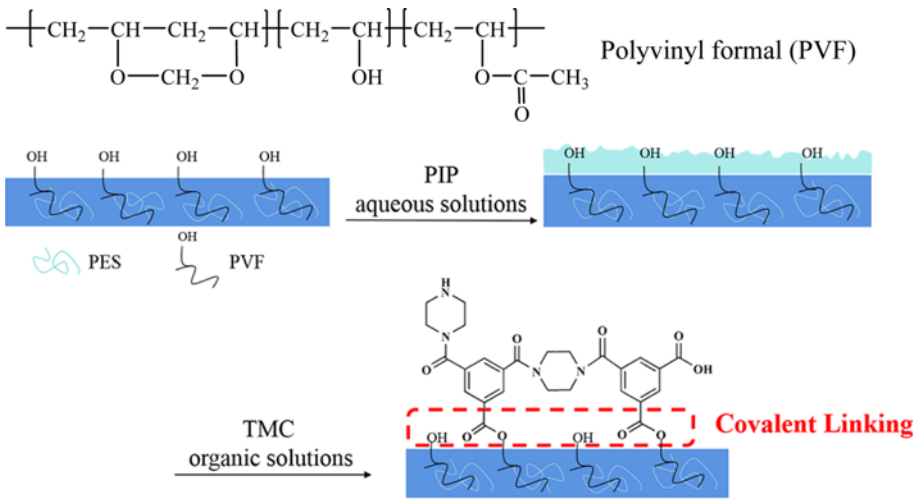

Fig. 1. Schematic illustration for the covalent linking between supports and interfacial polymerization layers of the composite nanofiltration membranes.

was further tested by long term immersion in ethanol.

Oligomeric proanthocyanidins (OPC) is a class of polyphenolic biflavonoids found in fruits and vegetables. OPC mainly exists in grape seeds and has been shown to protect against UV light-induced carcinogenesis and prevent immune suppression [16-18]. Concentration of OPC extract in ethanol solution is traditionally achieved by evaporation, which consumes considerable energy. As an alternative, the prepared composite NF membranes were employed for OPC concentration to allow the production of OPC at a lower cost. The resultant composite NF membranes offer a viable and sustainable alternate for energy-intensive evaporation processes during OPC concentration.

EXPERIMENTS

1. Materials

PES (6020P, Mw=29,000 Da) was purchased from BASF Co. (Germany). PVF (Mw=35 kDa) with an average acetalization degree of 80% was purchased from Tokyo Chemical Industry Co. (Japan). Both PES and PVF were dried at 70 °C for 24 h prior to use. Poly(ethylene glycol) (PEG, Mw=2,000 Da) was purchased from Damao Chemical Reagent Co. (Tianjin, China). N,N-dimethylformamide (DMF), PIP, n-heptane and ethanol were obtained from Guangfu Chemical Reagent Co. (Tianjin, China). TMC was purchased from Alfa Co. (USA). Sodium sulfate, orange GII and Congo red were purchased from J&K Scientific Ltd. (Beijing, China). OPC was purchased from Baoen Biotechnology Co. Ltd. (Hebei, China). Water used in all experiments was reverse osmosis water.

2. Preparation of PES-PVF Membranes and Composite NF Membranes

PES-PVF blend membranes were used as supports, which were prepared by non-solvent induced phase separation (NIPS). The casting solutions were prepared by dissolving PES and PVF into the organic solvent DMF at weight percentages of 10.0 and 6.0 wt%, respectively. The hydrophilic PVF was used as both pore-forming agent and modification agent. The pure PES membranes were prepared with 16 wt% PES and 16 wt% PEG in casting solution, while the hydrophilic PEG was used as pore forming. The detailed fabrication of support membranes was described in our previous works [11,19].

The composite NF membranes were prepared by interfacial polymerization of PIP with TMC. The support membranes were first immersed into aqueous solution of PIP. After being soaked for 30 min, excess solution on membrane surfaces was drained off by filter paper. Then the support membranes were immersed in TMC solution in n-heptane for a certain time at 25 °C to form the active layers by interfacial polymerization. After interfacial polymerization reaction, the membranes were taken out from organic solution and dried in the air for 10 min. Finally, the composite NF membranes were stored in water until they were tested. The composite NF membranes prepared with PES-PVF blend supports and pure PES supports were named PA/PES-PVF and PA/PES composite membranes, respectively.

3. Characterization of PES-PVF Membranes and Composite NF Membranes

The surface compositions of PES-PVF membranes were characterized by X-ray photoelectron spectroscopy (XPS, Perkin-Elmer PHI 1600 ESCA) with a monochromatic Mg Kα source and a charge neutralizer. To acquire thermal properties of the membranes, thermo gravimetric analysis (TGA, NETZSCH-TG209 F3) was conducted under nitrogen flow. Mechanical stabilities of the membranes were measured by an electronic stretching machine (Xinke WDW 3020) at a strain rate of 2 mm/min.

The surface morphologies of the composite NF membranes were observed with field emission scanning electron microscopy (FESEM, Nova Nanosem 430, FEI Co., USA). The membrane samples were dried in vacuum freeze dryer, and coated with gold before FESEM measurement.

Attenuated total reflection Flourier transformed infrared (ATR-FTIR) spectra of the prepared membranes were measured using an FTIR spectrometer (VERTEX 70, Bruker Co., Germany) equipped with both horizontal attenuated total reflectance accessories. Scans

were accumulated with a resolution of 4 cm^{-1} for each spectrum to investigate the functional groups on the membrane surfaces.

Contact angle goniometer (JC2000C Contact Angle Meter, Powereach Co., Shanghai, China) was used to measure the static contact angle of membranes at room temperature. At least six measurements on one surface were performed and the data were averaged to get a reliable value.

4. Separation Performance of Composite NF Membranes

The separation performance of the composite NF membranes was evaluated using a filtration cell (model 8200, Millipore Co., USA) equipped with a nitrogen gas cylinder and solution reservoir. The filtration cell has an inner diameter of 62 mm, effective area of 28.7 cm^2 and volume capacity of 200 mL. All the experiments were carried out at a stirring speed of 200 rpm and the feed side of the system was driven by nitrogen gas. Each membrane was initially compacted for about 30 min at 0.25 MPa to obtain a stable flux, then the pressure was dropped to the operation pressure of 0.20 MPa. The permeated flux (J, L/m^2h) was determined by measuring the permeated solution and calculated by the following equation:

$$J = \frac{V}{A\Delta t} \quad (1)$$

where V (L) is the volume of permeated solution during the experiment, A (m^2) is the membrane area, and Δt (h) is the operation time.

The filtration test cell was filled with aqueous solutions of inorganic salts or dyes to determine the rejections of the composite NF membranes. The concentration of inorganic salts and dyes in feed solutions was 1.0 and 0.1 g/L, respectively. The membrane rejection was characterized until the permeated fluxes and permeated salt or dye concentrations reached stable values. The rejection (R) was calculated by the following equation:

$$R = \left(1 - \frac{C_p}{C_f}\right) \times 100\% \quad (2)$$

where C_P and C_f are the inorganic salt or dye concentrations of the permeated and the feed solutions, respectively. The concentration of inorganic salts was measured by electrical conductivity (DDS-11A, Shanghai Leichi Instrument Co., Shanghai, China). The concentration of dyes was determined by a UV-vis spectrophotometer (Hitach UV-2800, Hitach Co., Japan). The wavelength of UV-vis spectrophotometer was adjusted to the maximum adsorption of dye solution in visible light range.

5. Structural Stability of Composite NF Membranes

The structural stability of the composite NF membranes was examined by ethanol treatment. PA/PES-PVF and PA/PES composite membranes were immersed in absolute ethanol for seven days to let the membranes become fully swollen; then the treated membranes were washed with an excess amount of water to remove any remaining ethanol. The influence of the immersion time on the water fluxes and rejection of the composite NF membranes was investigated. The properties of the membranes before and after ethanol treatment were measured through the aforementioned methods, and the stability of PA/PES-PVF and PA/PES composite membranes was evaluated according to the extent of performance deterioration after ethanol treatment.

Fluxes and rejections of orange GII by the prepared composite NF membranes for feed solutions with different ethanol content in water were examined to study the influence of ethanol on the performance of PA/PES-PVF composite membranes.

6. Concentration Experiments of OPC in Ethanol Solution

OPC used in this study was extracted from grape seeds. 1.0 g/L OPC content in ethanol solution with the initial feed volume of 200 mL was added into the cell for NF concentration. OPC content in the retained solution fraction (C_r) was calculated by the following equation:

$$C_r = \frac{V_0C_0 - V_tC_t}{V_0 - V_t} \quad (3)$$

where V_0 and V_t are the volume of the initial feed and the permeated solutions, respectively. C_0 is the OPC content in the initial feed solution, and C_t is the OPC content in the permeated solution at operation time of t moment. OPC content in feed and permeated solutions were analyzed with UV-vis spectrophotometer at a wavelength of 500 nm.

RESULTS AND DISCUSSION

1. Characterization of PES-PVF Membranes

The porous supports of PES-PVF blend membranes were first prepared. The theoretical value and XPS data of element contents of PES-PVF membrane was calculated (Fig. S1 and Table S1 in supporting information). The atomic ratio of O/S (8.92) in the membrane surface measured by XPS was higher than theoretical value of 4.08, indicating PVF was enriched on the membrane surface. The miscibility forecast of PES-PVF blend systems can be performed by the solubility parameter [20]. The solubility parameter calculated by group contribution theory for PES and PVF was 22.5 and 24.0 $MPa^{1/2}$, which indicated PES and PVF were partly compatible in theory [21] (Supporting information).

The thermal properties of the prepared PES-PVF membranes were evaluated by TGA (Fig. S2 in supporting information). The temperature at a 5% weight loss of PES-PVF membranes was 340.0 °C, while that of PES membranes was 305.0 °C. The results indicated the addition of PVF improved thermal stability of support membranes. The typical stress-strain curves for PES membranes and PES-PVF blend membranes were measured (Fig. S3 in supporting information); PES-PVF membranes had a better mechanical strength than PES membranes.

2. Characterization of Composite NF Membranes

Composite NF membranes have dense, ultrathin active layers upon porous supports, which lead to relatively high flux and low molecular weight cut off [22]. In this work, PES-PVF blend membranes were selected as supports, and the active layers were made by interfacial polymerization of TMC and PIP. PVF possessed pore formation and surface modification capabilities during the preparation of porous supports by NIPS method [11]. The water flux of PES-PVF blend membranes was 160.5±5.3 L/m^2h at pressure of 0.10 MPa.

ATR-FTIR spectra were first employed to analyze the functional groups on the near-surface region of PES, PES-PVF, and PA/PES-PVF composite membranes. In Fig. 2, beside typical bands of PES,

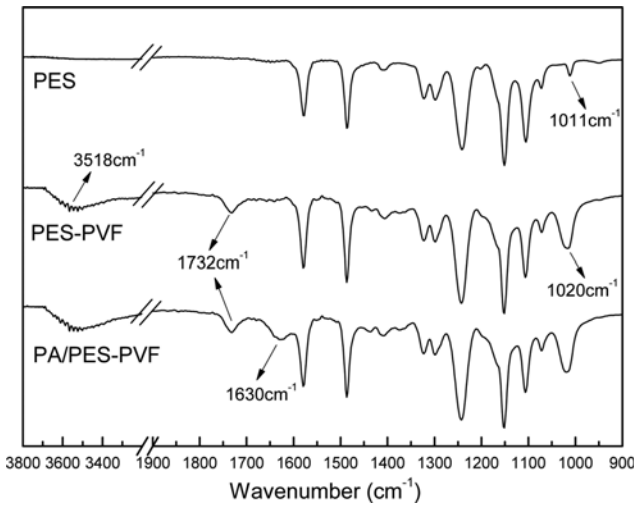

Fig. 2. ATR-FTIR spectra of PES membrane, PES-PVF blend membrane, and PA/PES-PVF composite membrane.

PES-PVF support membranes possessed additional peaks at 3,518 cm^{-1} and 1,732 cm^{-1}, which corresponded to the stretching vibration of hydroxyl groups and the C=O stretching vibration in ester bonds. Meanwhile, the spectra of PES-PVF support membranes exhibited a strong absorption peak at 1,020 cm^{-1}, which was assigned to the stretching vibration band of cycloaliphatic ethers. This stretching vibration band covered the absorption peak of aromatic ether at 1,011 cm^{-1} which belonged to PES. FTIR spectra verified the existence of PVF on the support membrane surfaces. Compared with PES-PVF support membranes, PA/PES-PVF composite membranes had additional peaks at 1,630 cm^{-1} (C=O stretching vibration in amide bonds), indicating that the PA active layers were successfully formed onto PES-PVF support membrane surfaces. The adsorption peak at 1,732 cm^{-1} of ester bonds between PA active layers and PES-PVF supports would coincide with non-hydrolyzed esters of PVF.

The surface and cross-section morphologies of composite NF membranes were observed by FESEM. Fig. 3 shows the SEM images of the top surface and cross-section morphologies of PES-PVF and PA/PES-PVF membranes. All the membranes displayed a typical asymmetric membrane morphology consisting of dense skin layers and porous support layers. There were observable pores on PES-PVF blend membrane surfaces (Fig. 3(A_1)) and the average pore size was about 20±5 nm due to PVF as pore forming agent. After interfacial polymerization, the membrane surfaces were dense without observable pores, and dispersed with nodular structures (Fig. 3(B_1)). Nodular structures on the surfaces of composite NF membranes mainly resulted from the cross-linking of PIP and TMC monomers. As shown in Fig. 3(B_3), a dense PA active layer was observed on the composite membrane after interfacial polymerization, which was about 86 nm thick. It was difficult to distinguish the PA active layer from the skin layer of support layer in PA/PES-PVF composite membrane, the modified support layer and the PA active layer had good adhesion with each other.

Water contact angle was commonly used to assess the hydrophilicity of membranes. In Fig. 4, the contact angle of PES-PVF blend supports (60.5±1.2°) is smaller than that of PES supports (68.1±2.1°), which was attributed to the enrichment of PVF on membrane surfaces increasing hydrophilicity of PES-PVF supports [11]. The PA/PES-PVF composite membranes had lower water contact angle compared with the supports due to the formation of hydrophilic PA active layers during the interfacial polymerization reaction. PA/PES and PA/PES-PVF composite membranes had nearly same static water contact angles before ethanol treatment. After

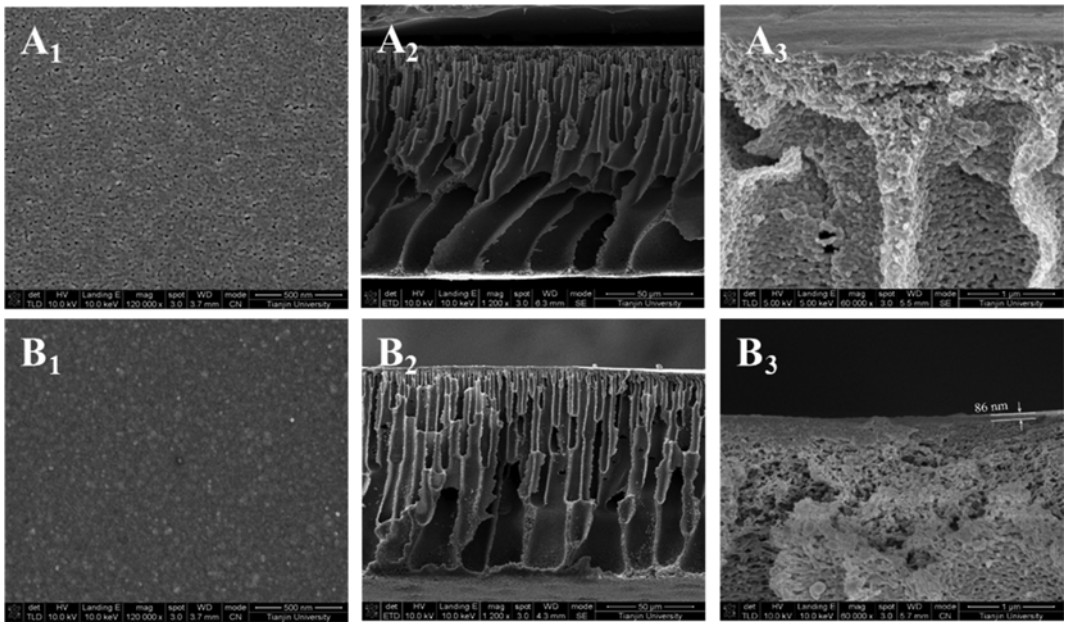

Fig. 3. SEM images of the top surface and cross-section morphologies of PES-PVF blend membranes (A_1, A_2 and A_3) and PA/PES-PVF composite membranes (B_1, B_2 and B_3).

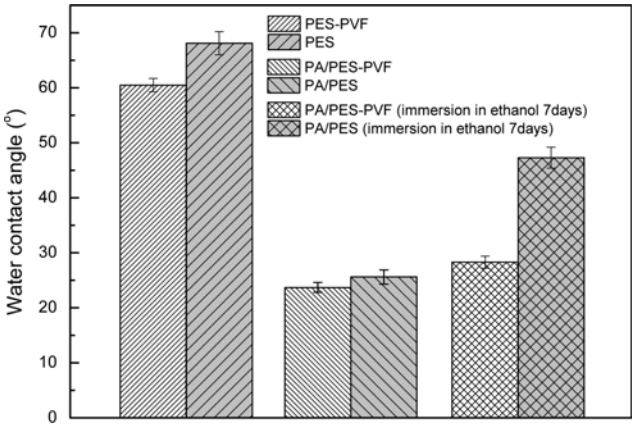

Fig. 4. Water contact angles of PES-PVF and PES memrbanes, PA/PES-PVF and PA/PES composite membranes before and after immersion in ethanol for 7 days.

immersing into ethanol for seven days, the water contact angle of PA/PES composite membranes increased from 25.6±1.3 to 47.3±1.9°. However, the water contact angle of PA/PES-PVF composite membranes just slightly increased from 23.7±0.9 to 28.3±1.9°. This indirectly revealed the structural stability of PA/PES-PVF composite membranes.

3. Effect of PIP and TMC Concentration on Membrane Performance

The separation performance of composite NF membranes is dependent on both preparation conditions and chemical structures [23]. The appropriate concentration of PIP in aqueous phase and TMC in organic phase for interfacial polymerization were investigated. Fig. 5 presents the effect of PIP concentration on fluxes and rejections of the composite NF membranes, while the TMC concentration was fixed at 0.20 wt% in organic phase and the interfacial polymerization time was fixed at 1 min. It was seen that the water fluxes decreased and the rejections increased continuously

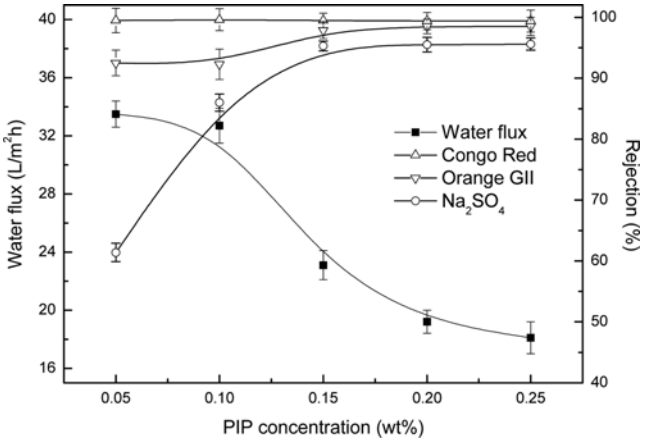

Fig. 5. Effect of PIP concentration in aqueous phase on fluxes and rejection of PA/PES-PVF composite membrane. TMC concentration in organic solution was fixed at 0.2 wt%. Interfacial polymerization reaction time was fixed at 1 min and the temperature was fixed at 20 °C. The filtration operation was carried out at a pressure of 0.20 MPa.

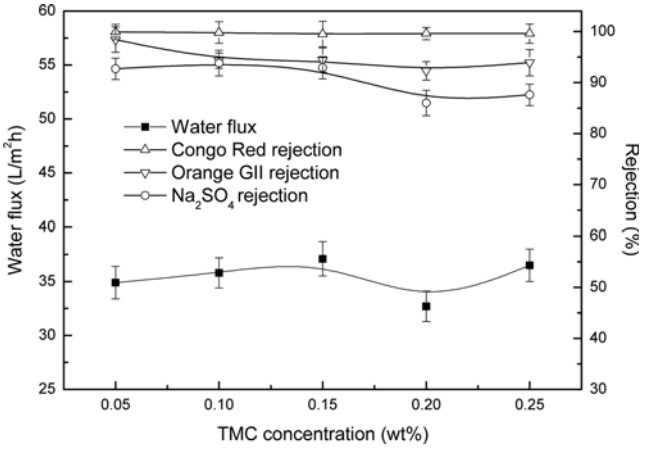

Fig. 6. Effect of TMC concentration in organic phase on fluxes and rejection of PA/PES-PVF composite membrane. PIP concentration in aqueous solution was fixed at 0.10 wt%. Interfacial polymerization reaction time was fixed at 1 min and the temperature was fixed at 20 °C. The filtration operation was carried out at a pressure of 0.20 MPa.

with increasing PIP from 0.05 to 0.25 wt%. The increase of PIP concentration in aqueous phase would lead to more PIP content diffusing into the water/oil interface and producing a dense active layer during interfacial polymerization process. But excessively high content of PIP was likely to be sterically hindered from interf, and therefore did not increase the density of the PA active layer [24]. According to the results shown above, the PIP concentration was fixed at 0.10 wt% in the following experiments.

Fig. 6 shows the effect of TMC concentration in organic phase on fluxes and rejection of PA-PES/PVF composite membranes. PIP concentration in aqueous solution was fixed at 0.10 wt% and the interfacial polymerization time was fixed at 1 min. The membrane performance was almost independent of the TMC concentration in organic phase. The probable reason was that the concentration of 0.05 wt% TMC in organic phase was enough to participate in the interfacial polymerization reaction. Both fluxes and rejection of Na_2SO_4 and orange GII of PA/PES-PVF composite membranes remained constant when further increasing the TMC concentration in organic solution. Therefore, it could be concluded that the PIP concentration in the aqueous phase played a dominant factor in affecting the membrane performance.

Based on the experiment data, the separation performance of PA/PES-PVF composite membranes was optimum, when the concentration of PIP was 0.10 wt% in aqueous phase and TMC was 0.05 wt% in organic phase, respectively. Water fluxes of PA/PES-PVF composite membranes could reach 34.9±1.5 L/m²h at operation press of 0.20 MPa, the rejection ratio of Na_2SO_4 was 92.7%, orange GII was 98.4%. Congo red was completely rejected by the composite NF membranes. This optimum preparation condition was used for the following experiments. Specially, the prepared PA/PES-PVF composite membranes in this study exhibited considerably high pure water fluxes and rejections, compared with other reported composite NF membranes (Table S2 in supporting information).

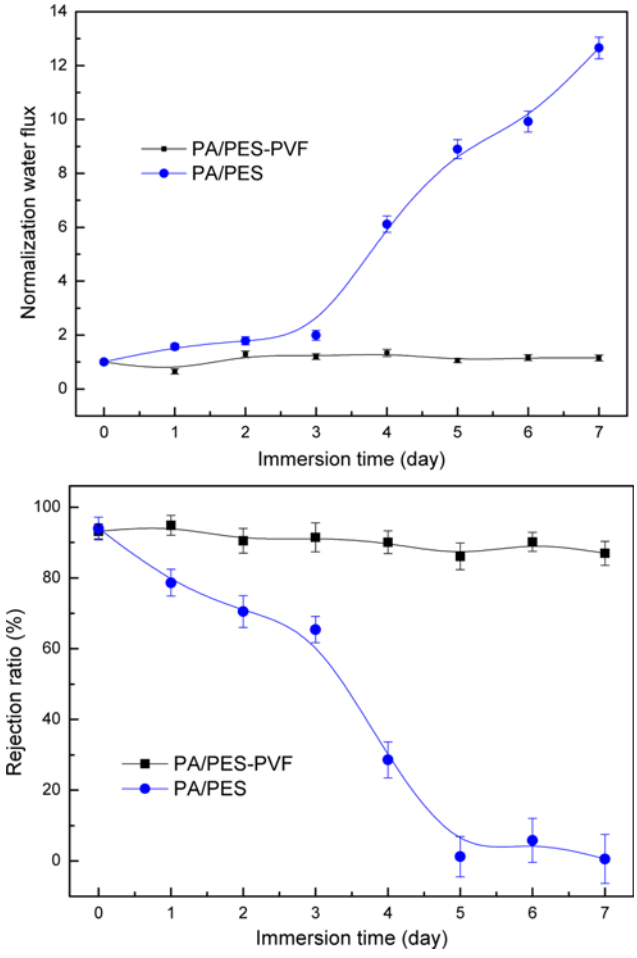

Fig. 7. The change of water fluxes and orange GII rejection for PA/PES and PA/PES-PVF composite membranes after immersion into pure ethanol. Orange GII concentrations in feed solutions was 0.1 g/L.

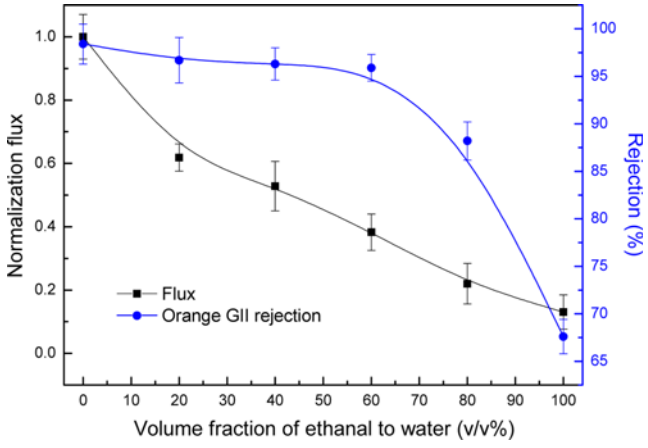

Fig. 8. The effect of ethanol concentration in feed solution on fluxes and rejection of orange GII of PA/PES-PVF composite membrane.

4. Structural Stability of Composite NF Membranes

In the actual operation, the structural stability was closely related to the lifespan of the composite membranes. To examine the structural stability of the composite NF membranes, PA/PES and PA/PES-PVF composite membranes were immersed into ethanol. Fig. 7 gives water fluxes and orange GII rejection of the composite NF membranes before and after immersing into ethanol for several days. The separation performance of PA/PES composite membranes seriously worsened. Water fluxes of PA/PES composite membranes increased more 12-fold and rejection of orange GII was decreased to 0.6%, after ethanol treatment for seven days. The swelling of the PES supports by ethanol might have caused the active layers to be detached from the supports, and resulted in higher water fluxes and poorer rejections. This could be interpreted that there was only physical adsorption between the active layers and PES supports. Therefore, PA/PES composite membranes had poor structural stability.

However, the water flux and rejection of PA/PES-PVF composite membranes had a little variation after immersing into ethanol for seven days. PA/PES-PVF composite membranes definitely had better structural stability than that of PA/PES composite membranes. The structural stability of PA/PES-PVF composite membranes might be attributed to the presence of the covalent linkage between the PA active layers and the supports. As explained before in Fig. 1, PES-PVF blend supports had hydroxyl groups on the surfaces, which could react with the carboxyl groups of TMC forming ester bonds between the active layers and the supports. Compared with the other modification methods in enhancing the structural stability of the composite membranes, this method has the advantage of simple production, which improve the structural stability just by blending method.

5. Separation Performance in Ethanol Solution

NF separation and concentration were gradually applied into organic solutions and aqueous solutions containing organic solutes. It was necessary to investigate the influence of organic content in water fluxes and rejections of composite NF membranes. Fig. 8 shows the effect of ethanol content in water-ethanol mixtures (feed solution) on fluxes and rejections of PA/PES-PVF composite membranes. It appears that both fluxes and rejections generally decreased with increasing ethanol content in water-ethanol mixtures. The flux of mixture with water-ethanol volume ratio of 6 : 4 was about 52.8% of pure water flux. The flux of pure ethanol was only 13.0% of pure water flux during NF operation. Viscosity and polarity of the mixture have large influence on the fluxes and rejections of composite NF membranes [25-27]. The viscosity of ethanol was higher than of water, which resulted in a higher viscous resistance against mass transport in both the active layers and supports.

The rejection of orange GII by PA-PES/PVF composite membranes in pure ethanol was only 67.6%, which was smaller than that in water (98.4%). Components in aqueous solution might be surrounded by a water shell that increased the effective size of the component, but there was no such effect for components in ethanol, the effective size might be lower, which should had a negative influence on the rejection. The rejection mechanism of NF membranes in ethanol was mainly determined by the molecular size (sieve effect) [28]. Therefore, the rejection of PA/PES-PVF com-

posite membranes in ethanol was smaller than that in water.

6. OPC Concentration in Ethanol Solution

Proanthocyanins of fruits and vegetables are potent free radical scavengers and believed to be of great benefit to health. OPC mainly exist in grape seeds, which have been shown to protect against UV light-induced carcinogenesis and prevent immune suppression [16-18]. Cyanidin and delphinidin are the basic structure units of grape seeds OPC, whose structure formula is shown in Fig. 9(a). Fig. 9(b) presents the conventional production process of OPC extracted from grape seeds. Macroporous resins are used to adsorb the crude OPC extraction and then eluted with water to remove the aqueous impurity. After washing by water, ethanol solution is used as medium to extract the adsorbed OPC from resins. The OPC extract in ethanol solution is concentrated and then dried by spray drying to obtain final OPC powder. Concentration of OPC extract in ethanol solution is traditionally achieved by evaporation, which consumes considerable energy. Hence there has been a need for an alternative technology that is more efficient both in terms of yield and energy consumption, in order to produce OPC at a lower cost.

NF concentration process is operated at ordinary temperatures, no phase transition, and low energy consumption [29]. NF membrane separation processes might have an improved efficiency and reduced operating cost in comparison with the traditional evaporation concentration processes. The prepared PA/PES-PVF composite membranes were used to concentrate the OPC ethanol solution with the operation pressure at 0.20 MPa. The initial feed solution contained 1.0 g/L OPC in ethanol solution (6 : 4 water/ethanol volume ratio). In the concentration processes, the rejection of OPC by PA/PES-PVF composite membranes was as high as 99.8%. There was nearly no loss of OPC during NF concentration process. Meanwhile, the permeated ethanol solution could be reused as medium to extract OPC from macroporous resin; this step further improved efficiency and saved energy.

Photographs of OPC initial feed solution, retained and permeated solutions are shown in Fig. 10; the retained solution was deep purple, while the permeated solution was colorless. The permeated fluxes decreased from 14.5 to 10.4 L/m^{2}h after operation time of 120 min due to concentration polarization and membrane fouling. The permeated flux remained at about 10.4 L/m^{2}h in the sequential concentration process. After finishing the concentration experiment, the volume of retained solution was about 1/20 of the initial feed solution, and the OPC content reached to 19.9 g/L in the final ethanol solution. The high OPC content ethanol solution by NF concentration could be directly dried by spray drying to obtain final OPC powder.

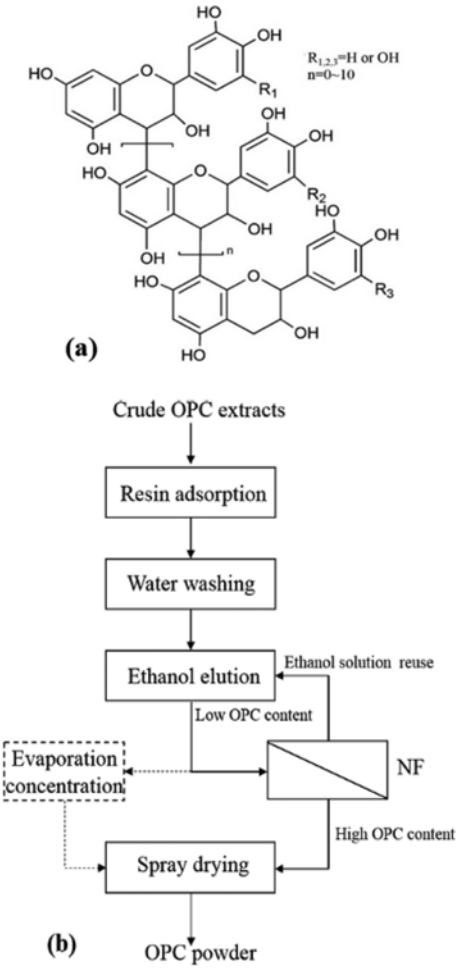

Fig. 9. (a) Structural formula of OPC. (b) The OPC extraction process from grape seeds by the traditional evaporation and nanofiltration concentration, respectively.

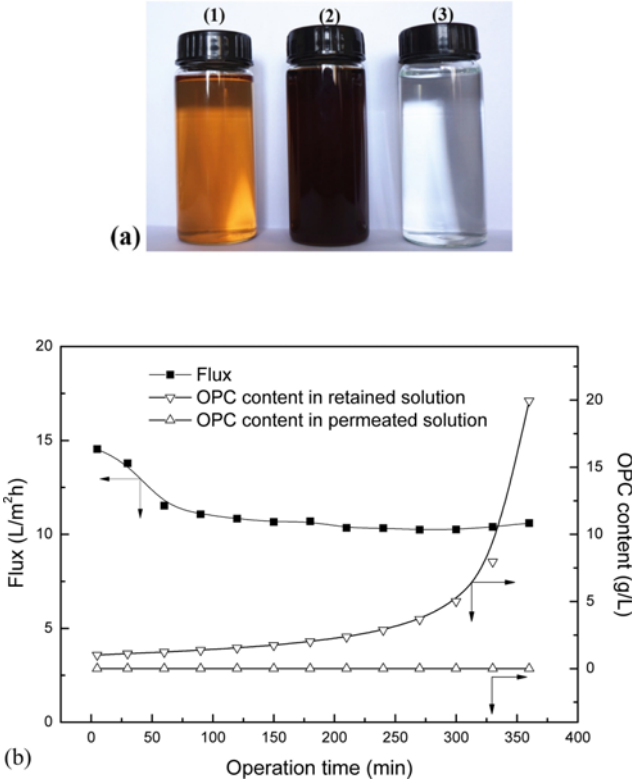

Fig. 10. (a) Photographs of OPC initial feed solution (1), retained (2) and permeated (3) solutions. (b) The permeated fluxes and OPC content in ethanol solution as functions of operation time during NF process. The initial OPC content was 1.0 g/L in feed ethanol solution.

CONCLUSIONS

PA/PES-PVF composite membranes were fabricated through interfacial polymerization of PIP and TMC on PES-PVF blend membranes. Hydroxyl groups of PVF, enriched on support membrane surfaces via surface segregation, could react with TMC and form ester bonds to chemically link active layers onto support membranes during interfacial polymerization. The prepared PA/PES-PVF composite membranes exhibited good structural stability after immersing in ethanol due to the strong interactions between the active layers and the PES-PVF blend membranes. PA/PES-PVF composite membranes were capable of concentrating OPC to a high content in ethanol solution with advantages of low energy consumption and solvent recycle, which had a potential to partially replace conventional evaporation process. Meanwhile, the composite NF membranes with enhanced structural stability would expand NF application in rugged environment.

ACKNOWLEDGEMENT

This research is supported by Tianjin Natural Science Foundation (No. 13JCYBJC20500, 14JCZDJC37400), National Science Fund for Distinguished Young Scholars (21125627).

SUPPORTING INFORMATION

Additional information as noted in the text. This information is available via the Internet at http://www.springer.com/chemistry/journal/11814.

NOMENCLATURE

OPC : oligomeric proanthocyanidins
PES : polyethersulfone
PVF : polyvinyl formal
PAN : polyacrylonitrile
PIP : piperazine
TMC : trimesoyl chloride
PA : polyamide
PEG : poly(ethylene glycol)
DMF : N, N-dimethylformamide
NF : nanofiltration
UF : ultrafiltration
RO : reverse osmosis
NIPS : non-solvent induced phase separation
J : flux [L/(m^2h)]
V : volume of permeated solution [L]
A : membrane area [m^2]
Δ_t : operation time [h]
R : rejection ratio [%]
C_p : solute concentration of permeate solution
C_f : solute concentration of feed solution
C_r : OPC content in retained solution
C_0 : OPC content in initial feed solution
C_t : OPC content in permeated solution at operation time of t moment
V_0 : volume of initial feed solution
V_t : volume of permeated solution at operation time of t moment

REFERENCES

1. C. Zhao, J. Xue, F. Ran and S. Sun, *Prog. Mater. Sci.*, **58**, 76 (2013).
2. M. Liu, S. Yu, Y. Zhou and C. Gao, *J. Membr. Sci.*, **310**, 289 (2008).
3. N. S. Kotrappanavar, A. A. Hussain, M. E. E. Abashar, I. S. Al-Mutaz, T. M. Aminabhavi and M. N. Nadagouda, *Desalination*, **280**, 174 (2011).
4. H. H. Himstedt, H. Du, K. M. Marshall, S. R. Wickramasinghe and X. Qian, *Ind. Eng. Chem. Res.*, **52**, 9259 (2013).
5. L. Huang, N. Bui, M. T. Meyering, T. J. Hamlin and J. R. McCutcheon, *J. Membr. Sci.*, **437**, 141 (2013).
6. J. Zhao, Y. Su, X. He, X. Zhao, Y. Li, R. Zhang and Z. Jiang, *J. Membr. Sci.*, **465**, 41 (2014).
7. B. Li, W. Liu, Z. Jiang, X. Dong, B. Wang and Y. Zhong, *Langmuir*, **25**, 7368 (2009).
8. H. I. Kim and S. S. Kim, *J. Membr. Sci.*, **286**, 193 (2006).
9. N. W. Oh, J. Jegal and K. H. Lee, *J. Appl. Polym. Sci.*, **80**, 2729 (2000).
10. J. Peng, Y. Su, W. Chen, X. Zhao, Z. Jiang, Y. Dong, Y. Zhang, J. Liu and X. Cao, *J. Membr. Sci.*, **427**, 92 (2013).
11. X. Fan, Y. Su, X. Zhao, Y. Li, R. Zhang, J. Zhao, Z. Jiang, J. Zhu, Y. Ma and Y. Liu, *J. Membr. Sci.*, **464**, 100 (2014).
12. X. Zhao, Y. Su, Y. Li, R. Zhang, J. Zhao and Z. Jiang, *J. Membr. Sci.*, **450**, 111 (2014).
13. A. M. Mayers and J. F. Hester, *J. Membr. Sci.*, **202**, 119 (2002).
14. X. Ma, Y. Su, Q. Sun, Y. Wang and Z. Jiang, *J. Membr. Sci.*, **292**, 116 (2007).
15. J. F. Hester, P. Banerjee and A. M. Mayes, *Macromolecules*, **32**, 1643 (1999).
16. B, Gabetta, N. Fuzzati, A. Griffini, E. Lolla, R. Pace, T. Ruffilli and F. Peterlongo, *Fitoterapia*, **71**, 162 (2000).
17. D. Ferreira and D. Slade, *Nat. Prod. Rep.*, **19**, 517 (2002).
18. C. Fu, A. E. K. Loo, F. P. P. Chia and D. Huang, *J. Agr. Food Chem.*, **55**, 7689 (2007).
19. J. Liu, Y. Su, J. Peng, X. Zhao, Y. Zhang, Y. Dong and Z. Jiang, *Ind. Eng. Chem. Res.*, **51**, 8308 (2012).
20. D. W. Van Krevelen and K. Te Nijenhuis, *Properties of polymers: Their correlation with chemical structure; their numerical estimation and prediction from additive group contributions*, 4th Ed., Elsevier, New York (2009).
21. Y. Peng and Y. Sui, *Desalination*, **196**, 13 (2006).
22. V. Freger, *Langmuir.*, **19**, 4791 (2003).
23. V. Freger and S. Srebnik, *J. Appl. Polym. Sci.*, **88**, 1162 (2003).
24. B. Tang, Z. Huo and P. Wu, *J. Membr. Sci.*, **320**, 198 (2008).
25. J. Geens, K. Peeters, B. Vanderbruggen and C. Vandecasteele, *J. Membr. Sci.*, **255**, 255 (2005).
26. S. Karan, S. Samitsu, X. Peng, K. Kurashima and I. Ichinose, *Science*, **335**, 444 (2012).
27. D. R. Machado, D. Hasson and R. Semiat, *J. Membr. Sci.*, **163**, 93 (1999).
28. B. Van der Bruggen,J. Geens and C. Vandecasteele, *Chem. Eng. Sci.*, **57**, 2511 (2002).
29. B. Pan, P. Yan, L. Zhu and X. Li, *Desalination*, **317**, 127 (2013).

Supporting Information

Fabrication of composite nanofiltration membranes with enhanced structural stability for concentrating oligomeric proanthocyanidins in ethanol aqueous solution

Yanyan Ma*,, Yanlei Su*,**,†, Yafei Li*,**, and Zhongyi Jiang*,****

*Key Laboratory for Green Technology of Ministry of Education, School of Chemical Engineering and Technology, Tianjin University, Tianjin 300072, China
**Collaborative Innovation Center of Chemical Science and Engineering (Tianjin), Tianjin 300072, China
(*Received 18 November 2014 • accepted 28 December 2014*)

1. Surface Enrichment of PVF

XPS (Fig. S1) analysis was performed to indicate the surface enrichment of PVF in the membrane. The atomic ratio was calculated and listed in Table S1. By the calculation, the theoretical atomic ratio of O/S in PES-PVF blend membrane was 4.08. The surface elemental mole percentages of the PES-PVF blend membranes were determined by XPS and the atomic ratio of O/S was 8.92. The surface atomic ratio of O/S was higher than the corresponding theoretical values, which indicated that PVF was enriched on the membrane surface.

2. The Miscibility of PES-PVF

The miscibility forecast of polymer blend systems can be performed by the solubility parameter (δ), which was calculated by group contribution theory. The corresponding equation for the solubility parameter is

$$\delta=\sqrt{\delta_d^2+\delta_p^2+\delta_h^2} \quad (1)$$

$$\delta_d=\frac{\sum F_{di}}{V} \quad (2)$$

$$\delta_p=\frac{\sqrt{\sum F_{Pi}^2}}{V} \quad (3)$$

$$\delta_h=\sqrt{\frac{\sum E_{hi}}{V}} \quad (4)$$

The solubility parameter calculated by group contribution theory for PES and PVF were 22.5 and 24.0 $MPa^{1/2}$, respectively [1]. When $|\delta_1-\delta_2|<1.0$ $MPa^{1/2}$, the polymer blends are completely miscible. When $1.0<|\delta_1-\delta_2|<3.5$-4.1 $MPa^{1/2}$, the blends are partly compatible [2]. Since $\delta_{PES}=22.5$ $MPa^{1/2}$, $\delta_{PVF}=24.0$ $MPa^{1/2}$, $1.0<|\delta_{PES}-\delta_{PVF}|=1.5<3.5$ $MPa^{1/2}$, PES and PVF were partly compatible in theory. Meanwhile, the casting solution of PES-PVF was kept glassy, never delaminated, which showed the blending system was macroscopical full miscibility.

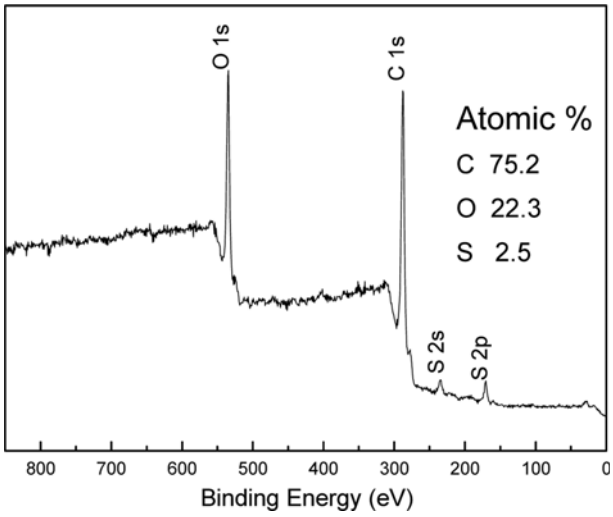

Fig. S1. XPS spectrum of PES-PVF membrane.

Table S1. Theoretical value and XPS data of PES-PVF membrane

	C (%)	O (%)	S (%)	Atomic ratio of O/S
Theoretical value[a]	74.24	20.69	5.07	4.08
XPS data	75.20	22.30	2.50	8.92

[a]The theoretical value was calculated based on the composition of PES-PVF membrane casting solution

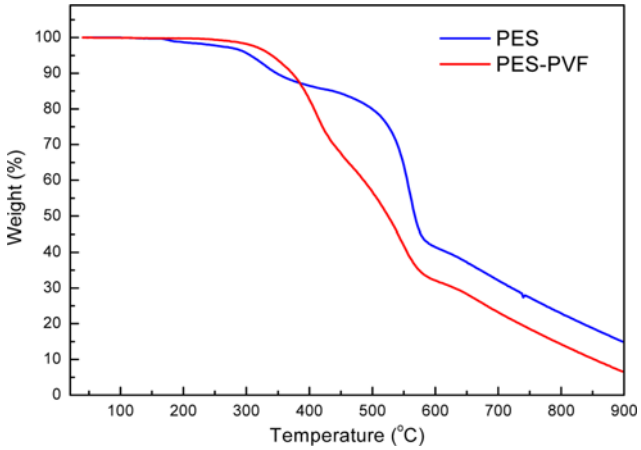

Fig. S2. TGA curves of PES membranes and PES-PVF blend membranes.

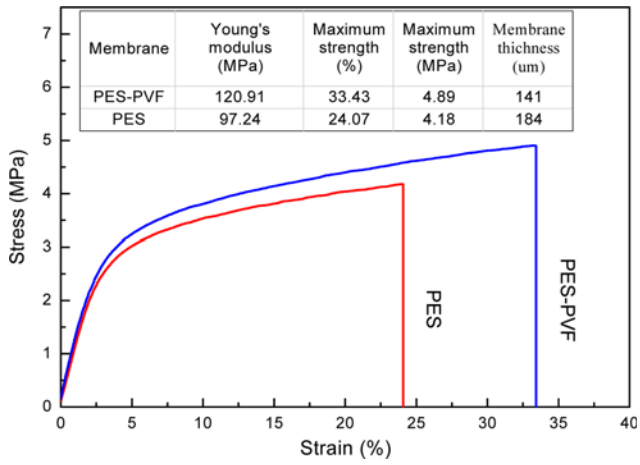

Fig. S3. Stress-strain curves of PES membranes and PES-PVF blend membranes.

Table S2. The comparison of NF performance

Water flux	Rejection	Operating pressure	References
34.9±1.5 L/(m^{2}h)	Na_2SO_4 92.7% Orange GII 98.4% Congo Red 99.9%	0.2 MPa	This work
22.8 L/(m^{2}h)	Na_2SO_4 93.5% Mg_2O_4 81.0%	0.2 MPa	[3]
10.0 L/(m^{2}h)	Na_2SO_4 53.0% $MgSO_4$ 91.0%	0.6 MPa	[4]
5.0 L/(m^{2}h)	Na_2SO_4 54.9% $MgSO_4$ 52.3% $MgCl_2$ 20.0%	0.6 MPa	[5]
43.1 L/(m^{2}h)	K_2SO_4 97%	0.6 MPa	[6]
36 L/(m^{2}h)	Direct red 99%	0.4 MPa	[7]
36.6 L/(m^{2}h)	$MgCl_2$ 95%	0.1 MPa	[8]
128.5 L/(m^{2}h)	Brilliant blue 100% Congo red 99.7% Methyl orange 22.7%	0.4 MPa	[9]
68.2 L/(m^{2}h)	Na_2SO_4 58.2% $MgSO_4$ 85.1%	0.6 MPa	[10]

3. Thermal and Mechanical Properties of PES-PVF Membrane

The thermal properties of the prepared composite NF membranes were evaluated by TGA instruments (NETZSCH-TG209 F3) under nitrogen flow. The TGA curves of PES membranes and PES-PVF membranes were shown in Fig. S2. The temperature at a 5% weight loss of PES-PVF membranes was 340.0 °C, while that of PES membranes was 305.0 °C. The results indicated the addition of PVF improved thermal stability.

Mechanical stabilities of the membranes were measured by an electronic stretching machine at a strain rate of 2 mm/min. The typical stress-strain curves for PES membranes and PES-PVF membranes were plotted in Fig. S3 and the mechanical property data and membrane thickness were presented in the table. The results exhibited PES-PVF membranes had a better mechanical strength.

4. Comparison of NF Performance

The comparisons in flux and rejection between the prepared membranes and ever reported/existed membranes were provided in Table S2. For the prepared PA/PES-PVF composite membrane, the water flux could be as high as 34.9 L/(m^{2}h), at operation press of 0.2 MPa, the rejection ratio of Na_2SO_4 was 92.7%, orange GII was 98.4%. Congo red was completely rejected by the composite membranes. Through these comparisons, PA/PES-PVF composite membrane had considerably high pure water flux and permeation.

NOMENCLATURE

δ : the total solubility parameter [MPa$^{1/2}$]
δ_d : contribution of dispersion forces to the solubility parameter [MPa$^{1/2}$]
δ_p : contribution of polar forces to the solubility parameter [MPa$^{1/2}$]
δ_h : contribution of hydrogen bonding to the solubility parameter [MPa$^{1/2}$]
F_d : dispersion component of the molar attraction function [(MJ/m^3)$^{1/2}$ mol^{-1}]
F_p : polar component of the molar attraction function [(MJ/m^3)$^{1/2}$ mol^{-1}]
E_h : contribution of the hydrogen bonding forces to the cohesive energy [J/mol]
V_m : molar volume [cm^3/mol]

REFERENCE

1. D. W. Van Krevelen and K. Te Nijenhuis, *Properties of polymers: Their correlation with chemical structure; their numerical estimation and prediction from additive group contributions*, 4th Ed., Elsevier, New York (2009).
2. Y. Peng and Y. Sui, *Desalination*, **196**, 13 (2006).
3. Y. Li, Y. Su, J. Li, X. Zhao, R. Zhang, X. Fan, J. Zhu, Y. Ma, Y. Liu and Z. Jiang, *J. Membr. Sci.*, **476**, 10 (2015).
4. Y. Lv, H. Yang, H. Liang, L. Wan and Z. Xu, *J. Membr. Sci.*, **476**, 50 (2015).
5. B. Tang, Z. Huo and P. Wu, *J. Membr. Sci.*, **320**, 198 (2008).
6. Q. An, W. Sun, Q. Zhao, Y. Ji and C. Gao, *J. Membr. Sci.*, **431**, 171 (2013).
7. S. Zinadini, A. A. Zinatizadeh, M. Rahimi, V. Vatanpour, H. Zangeneh and M. Beygzadeh, *Desalination*, **349**, 145 (2014).
8. X. Li, R. Wang, F. Wicaksana, C. Tang and J. Torres, *J. Membr. Sci.*, **450**, 181 (2014).
9. X. Li, L. Zhu, B. Zhu and Y. Xu, *Sep. Purif. Technol.*, **83**, 66 (2011).
10. L. Li, B. Guo, H. Tan, T. Chen and J. Xu, *J. Membr. Sci.*, **269**, 84 (2006).